

Design of the photomultiplier bases for the surface detectors of the Pierre Auger Observatory

B. Genolini, T. Nguyen Trung, J. Pouthas, I. Lhenry-Yvon, E. Parizot, T. Suomijarvi

► **To cite this version:**

B. Genolini, T. Nguyen Trung, J. Pouthas, I. Lhenry-Yvon, E. Parizot, et al.. Design of the photomultiplier bases for the surface detectors of the Pierre Auger Observatory. 2001, pp.10. in2p3-00009946

HAL Id: in2p3-00009946

<http://hal.in2p3.fr/in2p3-00009946>

Submitted on 2 Jul 2001

HAL is a multi-disciplinary open access archive for the deposit and dissemination of scientific research documents, whether they are published or not. The documents may come from teaching and research institutions in France or abroad, or from public or private research centers.

L'archive ouverte pluridisciplinaire **HAL**, est destinée au dépôt et à la diffusion de documents scientifiques de niveau recherche, publiés ou non, émanant des établissements d'enseignement et de recherche français ou étrangers, des laboratoires publics ou privés.

DESIGN OF THE PHOTOMULTIPLIER BASES FOR THE SURFACE DETECTORS OF THE PIERRE AUGER OBSERVATORY

B. Genolini, T. Nguyen Trung, J. Pouthas,
I. Lhenry-Yvon, E. Parizot, T. Suomijärvi

Corresponding author: B. Genolini - <mailto:genolini@ipno.in2p3.fr>

Institut de Physique Nucléaire d'Orsay
91406 Orsay Cedex, France

ABSTRACT

The design of the photomultiplier bases for the surface detectors of the Pierre Auger Observatory is presented. The bleeder is purely resistive. The base comprises two outputs: one from the anode, and another one from the last dynode followed by an amplifier. The charge ratio between the anode and the amplified dynode is around 30. The design ensures a low consumption (less than 100 μ A at 2 kV), a stability of the gain and of the base line during the whole period of measurement (20 μ s per event) and for the whole dynamic range (max. 1 to 3×10^4 in amplitude). First measurements with a prototype base on the Hamamatsu R5912 photomultiplier tube are presented.

1. INTRODUCTION

The surface detectors of the Pierre Auger Observatory [1] are designed to measure particle showers created by cosmic rays with energies of up to 10^{21} eV. The surface array is composed of 1,600 Cerenkov water tanks placed on a grid with a spacing of 1.5 km. The ground particles of the shower (mainly photons, electrons and muons) are detected through the emission of the Cerenkov light induced by these particles in the water. The Cerenkov light is detected by three photomultiplier tubes (PMTs) placed on the top of each tank. The PMTs have to measure signals over a wide dynamic range of amplitude and charge because of the large variation of the particle density with the primary energy and the distance between the shower core and the tank [2]. Since the surface detectors are supplied with solar cell batteries, the PMT bases have to fulfill stringent constraints on the power consumption.

This document briefly presents the requirements that guided and constrained the base design. A description of the base with justifications of the technical choices, and the results of the first measurements with a base prototype are also presented.

2. REQUIREMENTS

Based on the shower simulations of Ref. [2], the largest signals to be considered correspond to a peak photocathode current i_{Kmax} of around 300 nA, a 10-90 % rise time of around 100 ns, a 90-10 % fall time of around 500 ns, for a total charge of 6×10^5 photoelectrons. The minimal signal to be measured is that of a few photoelectrons. The simulations and measurements on a tank [3] show that the average of a single muon signal has an exponential shape with a decay time constant of around 50 ns and a number of photoelectrons around 30. The rate of events in a tank is around 2 kHz, coming mainly from individual muons. As a consequence, the mean photocathode current is very low: 10 fA.

The maximum signal to handle and the expected limit of the PMT linearity (60 mA) lead to a standard operating gain of 2×10^5 . In the PMT specifications, the operation mode is required to be extended to 10^6 in order to have more flexibility in the adjustment of the dynamic range. With the standard gain of 2×10^5 the average amplitude for a single photoelectron anode signal on a 50Ω impedance is around $200 \mu\text{V}$ (for a standard pulse shape with a 10 ns FWHM). In order to ensure a good signal to noise ratio after the transmission through the cables to the front-end electronics, a local amplification is mandatory.

The PMT cathodes are placed near the water and therefore the PMTs have to be supplied with a positive high voltage. The maximum high voltage will be 2 kV and has to be provided locally from a module powered with a +12 V DC. The power for the amplifiers is taken from +3.3 and -3.3 V regulated supplies. The total power budget for one PMT base is limited to 500 mW i.e. 1.5 mW per tank. The specifications for the high voltage supplies are given in appendix A.

3. BASE DESIGN

In order to match the dynamic range, the PMT base has two outputs: one from the anode, and the other one from an amplifier connected to the last dynode. The final choice of the PMT is foreseen on summer 2001. Three companies are delivering prototypes: R5912-MOD (8 dynodes) by Hamamatsu, XP1805 (8 dynodes) by Photonis, and D731 (10 dynodes) by ETL. The principle of the base design is the same for the different kinds of PMTs. The major change between the different bases is the voltage distribution that is given by the constructors. The parameters that determine the design are the gain and the base line stability during the occurrence of large pulses. We have made bases for two of the prototypes delivered for the Engineering Array: Photonis XP1802 (11 stages) and the Hamamatsu R5912 (10 stages). The design presented here concerns the R5912.

3.1 Description

The schematics of the base is presented in Figure 1. The design relies only on resistors and capacitors. The voltage distribution on the electrodes of the PMT is tapered in order to improve the linearity of the PMT [4-6]. The signal pickup of the last dynode relies on the standard scheme [4], but with a higher value for the isolation resistance R_{IN} , which will be justified below.

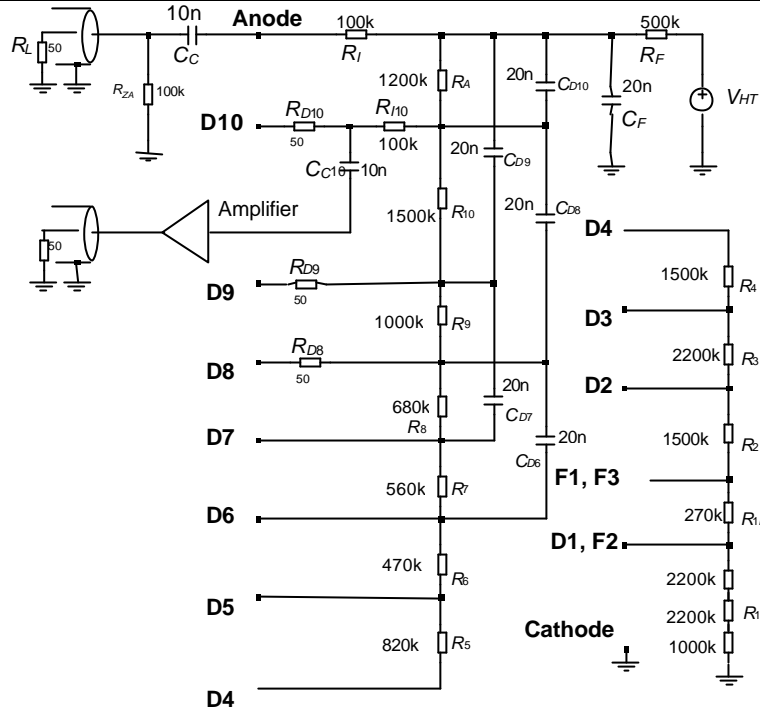


Figure 1 Schematics of the base developed for the R5912. Decoupling capacitors have a semi-parallel geometry to facilitate the implementation on the printed circuit board. Damping resistors (R_{Dk}) are placed on the last stages to reduce the ringing due to the parasitic inductances of the PMT inner leads.

For our tests the bias current was chosen to be $60 \mu\text{A}$ at the operating gain. This value is considerably larger than the standard recommendations (bias current greater than 100 times the anode current at all the operating gains and taking into account the voltage dispersion [4, 5]). However an important reduction of the bias current would mean to use resistances above $10 \text{ M}\Omega$ to define the dynode potentials. At this order of magnitude, the circuit is more sensitive to leakage currents that would create non negligible fluctuations of the dynode potentials and there is less choice in the values of components.

3.2 Gain stability

The gain is determined by the value of each dynode potential, whose variations depend mainly on the current pulses that flow through the base components. The equivalent model for the base in pulse mode is presented in Figure 2. Using the standard formulae [4, 5], the relative gain variation g_k associated to the k -th dynode (k ranging from 1 to N , where N is the number of dynodes) for a small relative variation of the potential V_k of this dynode can be calculated from the logarithmic derivatives:

$$\frac{dg_k}{g_k} = a \frac{dV_k}{V_k} \quad (1)$$

where a can be considered as constant for all the stages. Depending on the PMT, a ranges from 0.6 to 0.8 [4, 5]. As a consequence, if the relative voltage variation is the same for N stages (e.g. a variation of the high voltage supply), the global relative variation will be N times the variation on a single stage, since the total gain is the product of all the intermediate gains g_k .

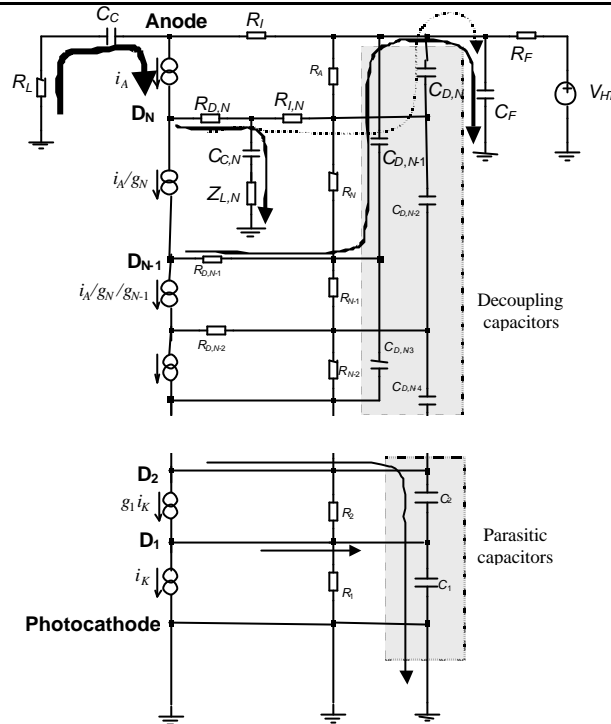


Figure 2 Equivalent model for the main current paths in pulse mode. The amplifier is represented by its input impedance Z_{LN} .

At the maximum current of 60 mA, the anode potential variation is due to the current pulse crossing the impedance of the cable R_L , and is 3 V at maximum. This value is less than 5 % of the nominal potential difference between the anode and the last dynode, and should have a negligible impact on the gain. The voltage drop due to the total charge of the greatest pulses crossing the capacitor C_C is less than 300 mV, due to the large value of this capacitor. The effect of the anode current has a minor impact on the PMT gain, since the anode is a non-amplifying electrode, and because it is isolated from the dynodes by the isolation resistance R_I .

The current of the last dynode crosses the damping resistance R_{DN} (50 Ω), the coupling capacitance $C_{C,N}$ and the impedance of the amplifier, represented by Z_{LN} . The main voltage variation is due to the peak current through the whole impedance ($R_{DN} + Z_{LN}$ in pulse mode), which is around 70 Ω for the largest pulses because Z_{LN} is reduced to around 20 Ω by the protection at the input of the amplifier (see below). A small part of the last dynode current flows through the isolation resistance R_{IN} and is evacuated through the capacitors $C_{D,N}$ and C_F . It results in negligible potential variations in the voltage divider. As a consequence, even if the voltage variation on the last dynode is estimated to 3 V, a calculation using formula (1) leads to an estimate of a gain variation less than 1 %.

For the pulses coming from the other dynodes, the path of the pulses depend on the position of the dynode: for the first dynodes, the pulses go to the ground via the parasitic capacitances which have an order of magnitude of 1 pF. The voltage variation, caused mainly by the charge variation on these capacitances, is negligible for these stages. Concerning the last stages, the pulses cross the decoupling capacitors (see Figure 1) and the capacitor of the voltage supply filter C_F . The filter resistance R_F ensures that a negligible reverse current goes through the high voltage supply. With values of 20 nF for the decoupling capacitors, and 10 nF for the filter capacitor, calculations using formula (1) show that the voltage variations that are due to the largest pulses have a negligible impact on the gain (less than 1 %).

3.3 Base line stability

After each pulse, there is a recovery process that compensates the charge variations in the capacitors. The associated currents that cross the readout impedances are responsible for the base line variations. A model presenting the main recovery currents is shown in Figure 3. The limitation of these currents is achieved through large time constants.

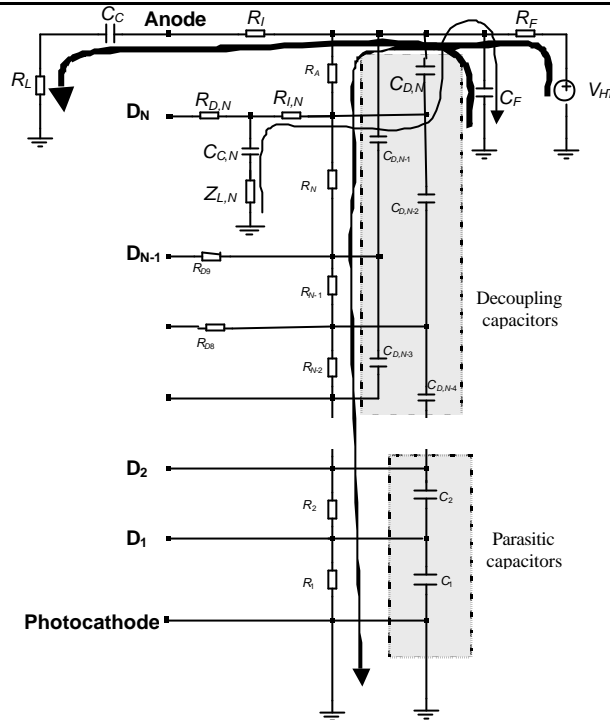


Figure 3 Model for the main current paths in the base during the recovery of the capacitors

The refilling time of the anode coupling capacitor C_C is mainly determined by R_I and R_F and the capacitances C_C and C_F . This yields time constants around 2 ms and a base line variation for the largest pulses less than 0.5 mV. Due to the gain of the amplifier, the recovery current of the coupling capacitance of the last dynode $C_{C,N}$ has a larger influence on the base line. The recovery process has two time constants: the first one to fill the C_F capacitor (loop made by $C_{C,N}$, $R_{I,N}$, C_N , C_F), and the second one to empty this capacitor through the whole resistance of the divider. This leads to a time constant of the second process which is seven times greater than the first one. With the current design, the base line variation is 20 mV for the largest pulses with a value of 100 k Ω on $R_{I,N}$. The value of $R_{I,N}$ should be increased to limit the base line variations to 2 mV on the largest pulses. However, the pulses to consider on the dynode output have a charge at least ten times lower which would lead to a base line fluctuation less than 2 mV.

3.4 Amplification of the dynode signal

The desired charge ratio between the two outputs of the base is around 30. The gain of the amplifier must take into account the following relationship between the anode current i_A and the last dynode current i_{DN} :

$$i_{DN} = \left(1 - \frac{1}{g_N}\right) i_A$$

where g_N is the gain of the last dynode [4, 5]. With the values given by the constructor g_N is around 3. Therefore i_{DN} is around 0.7 i_A . To get a charge ratio of 30 between the two outputs, the transimpedance of the amplifier must be around $2 \times 10^3 \text{ V} \cdot \text{A}^{-1}$.

The schematics of the amplifier is presented in Figure 4. It comprises two stages, based on the same operational amplifier, the AD 8011. The transimpedance of the first stage is $-R_{F1}$. According to the constructor recommendations, the value of R_{F1} (500 Ω) is the minimal value allowed to operate with the largest bandwidth. The capacitors C_{F1} and C_{F2} have the minimal value recommended by the constructors (1 pF) to stabilize the amplifier. Capacitors C_{L1} and C_{L2} are needed to suppress the offset of the amplifiers. The base line variation induced by the differentiation is limited by using large values for these capacitors (4.7 μF). A limitation of the current at then input amplfier is achieved by diodes (circuit BAS70-04). The maximum current is 14 mA, determined by the threshold of the diode (0.7 V) and the input resistor R_{G1} (50 Ω).

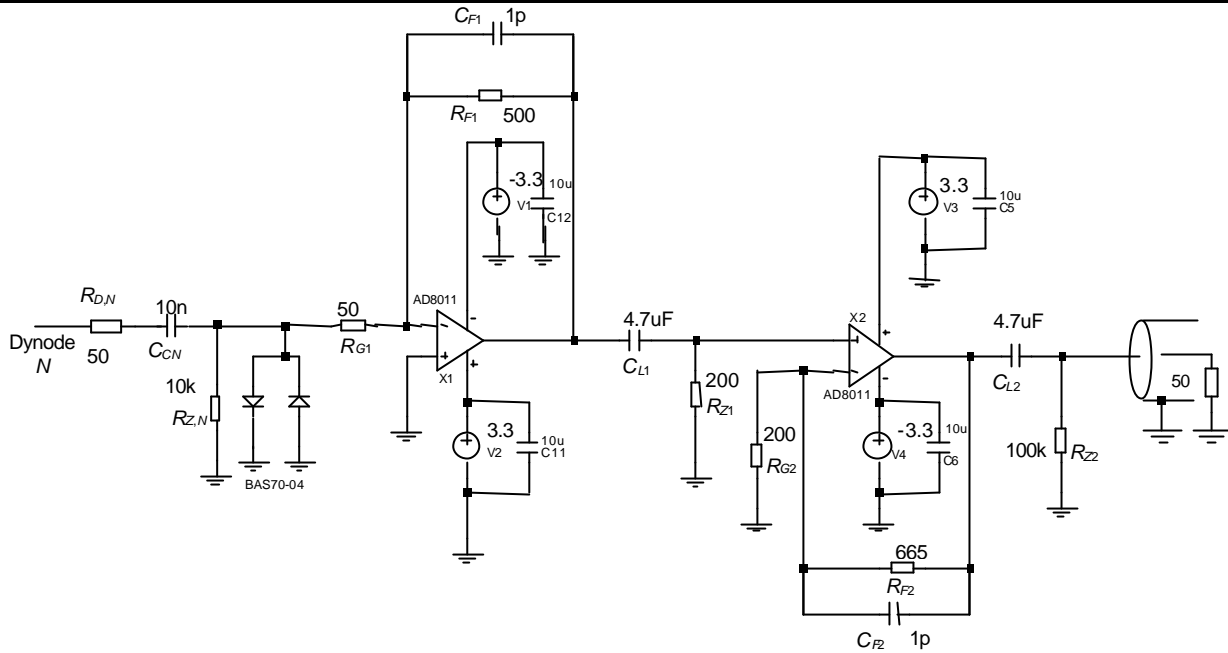


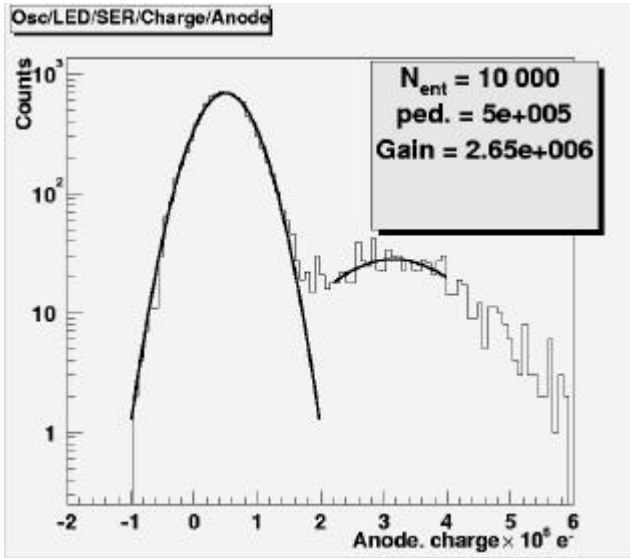
Figure 4 Schematics of the dynode amplifier.

3.5 About the possible use of transistors

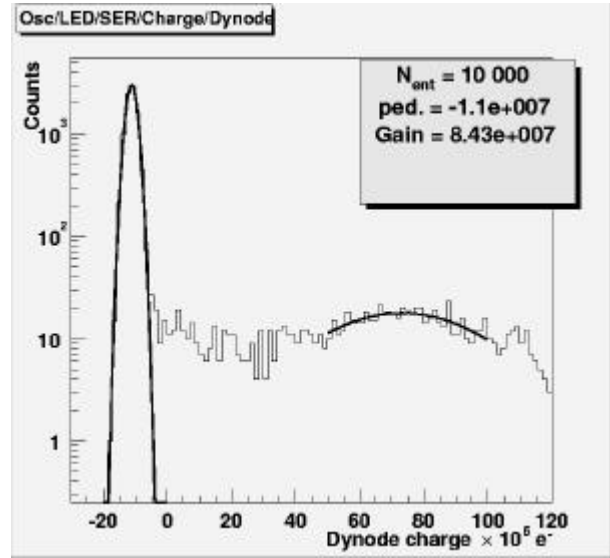
Due to the very low counting rate and average current, the use of transistors in the base is not necessary. N type transistors (NPN or NMOS) are typically used to stabilize the dynode potentials when it is necessary to work with an important average current [4-7]. They are put in parallel with the decoupling capacitors, on the last stages. In case of applications with a high counting rate, these transistors may reduce the refilling time of the decoupling capacitors by a factor greater than 10 [8, 9]. The only interest of transistors would have been to help the evacuation of the charge of pulses, working as common base (or common gate) amplifiers. With an architecture relying on N type transistors on the last stages, this could not work because this would mean a reverse current through the N-type transistors much greater than the bias current. Therefore, we would have to use a fully P-type (PNP or PMOS) transistorized base. However the existing PMOS transistors that could produce a sufficiently high current need a relatively important bias current, or have bandwidth limitations. The other drawback of such a design is the cost and the reliability in comparison with a purely resistive base.

4. FIRST RESULTS

First results were obtained on the Hamamatsu R5912 10 stage PMT. All the measurements were performed with a Tektronix TDS 580D digitizing oscilloscope, sampling the signals with an equivalent 9 bit flash ADC at a maximum sampling rate of 4 GSPS. The base was operated with a bias current of $58 \mu\text{A}$ and with a high voltage of 1000 V. The gain of the PMT was 2.7×10^6 . The calibration was performed with a LED pulsed by a 3 ns FWHM wide signal. The single electron signals on the anode have an amplitude of around 3 mV and a FWHM around 6 ns. The histograms of single electron response on the two outputs of the base are presented in Figure 5. The ratio in charge measured on the two outputs is 32.



Single electron charge spectrum on the anode



Single electron charge spectrum on the amplified dynode

Figure 5 Single electron response for the Hamamatsu R5912 with the base prototype. The measurements were performed with a digitizing oscilloscope. The signals were digitized over a 125 ns window comprising 500 points.

The LED was also used to check the linearity between the anode and the dynode outputs. The results are presented in Figure 6. A good linearity is observed between the anode and the dynode up to the saturation of the amplifier which occurs at 1.2 V. A non linearity is observed at the same level for the charge. In the linear range, the charge ratio between the two outputs is 33. The limit of the linear range on the dynode is 2×10^9 electrons. The amplitude ratio between the two outputs is only 28 because of the integration performed by the dynode amplifier.

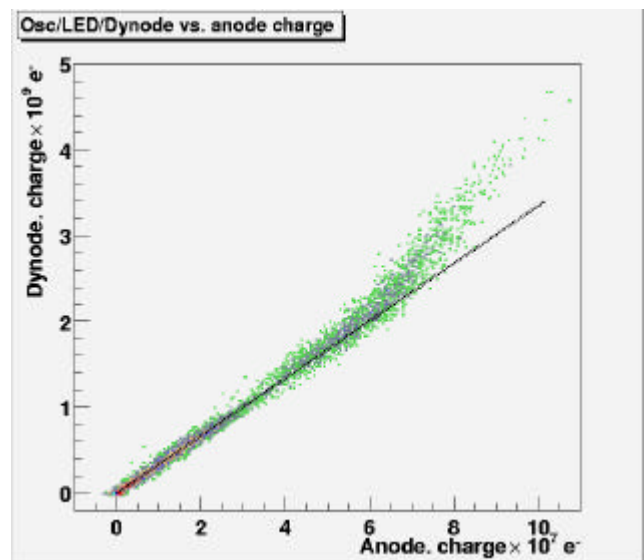
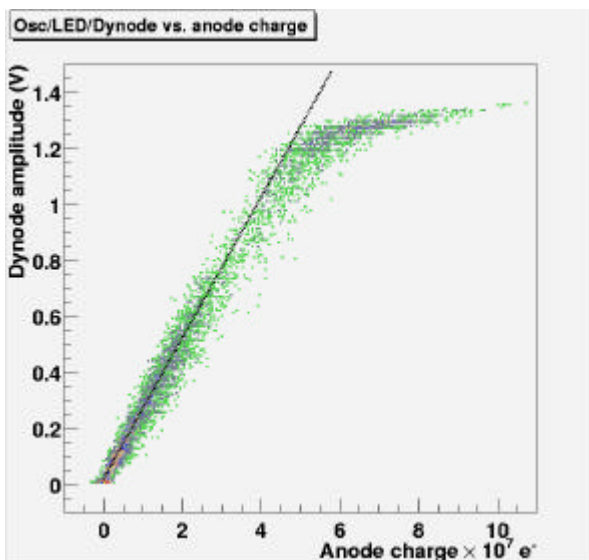
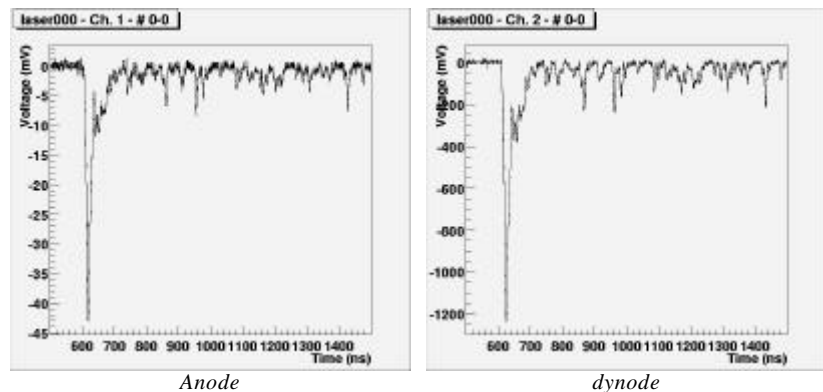


Figure 6 Linearity measured on a R5912 PMT operated at a gain of $2.7 \cdot 10^6$. Correlation between the charge measured on the dynode and the charge measured on the anode with a digitizing oscilloscope. The signals were digitized over a 125 ns window comprising 500 points. This plot is the collection of measurements with several values on the command corresponding to 1.5, 8, and 21 photoelectrons in average. This low number of photoelectrons leads to a charge dispersion which allow to cover the dynamic range.

A second set of measurements was performed to test the behavior of the dynode output after the saturation. A 337 nm Nitrogen laser exciting a CsI(Tl) cristal was used. A filter was placed between the cristal and the

PMT to attenuate the fast laser light and to measure on long time ranges [10]. The measurements, presented in Figure 7, show the short recovery of the amplifier after a saturation of 5 times its linear limit.

Anode and dynode signals measured on the Same event, close to the limit of the linear range of the amplifier



Anode and dynode signals measured on the Same event, when the pulse exceeds by a factor of 5 the linear range of the amplifier.

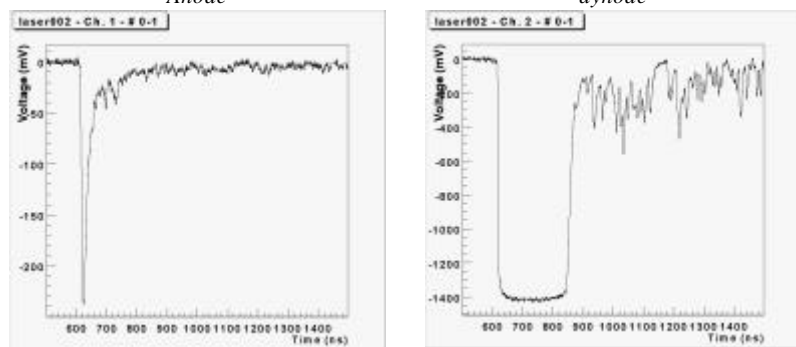


Figure 7 Comparison of the anode and dynode outputs with and without saturation of the dynode amplifier. The PMT is a Hamamatsu R5912 working at a gain of $2.7 \cdot 10^6$. The sampling rate is 1 GSPS.

5. CONCLUSION

A purely resistive low power base has been designed. It comprises two outputs: direct anode and last dynode through an amplifier. The charge ratio between the two outputs is around 32. The measurements performed with a prototype show a good linearity between the two outputs and a short recovery time of the amplifier after the saturation which occurs at 1.2 V. In the future, other low-power amplifiers will be considered in order to increase the saturation limit.

6. REFERENCES

- [1] The Pierre Auger Project Design Report, November 1996, <http://www.auger.org>
- [2] I. Lhenry-Yvon et al., *Surface Detectors Electronics of the Pierre Auger Observatory: simulations on the dynamic range*, IPNO DR-01-009, GAP note in preparation, 2001, and references therein.
- [3] INFN Torino and IPN-Orsay, *Measurements on the Galpon tank in November 2000*, GAP note in preparation, 2001
- [4] Philips Photonics (Photonis), *Photomultiplier tubes, principles and applications*, <http://www.photonis.com>, 1994
- [5] Hamamatsu Photonics K. K., *Photomultiplier tubes - principle to application*, Hamamatsu Photonics K. K. - Electron tubes center, 1994

-
- [6] Y. Yoshizawa et al., *The study of Countrate Stability of Photomultiplier Tube with Different types of Voltage Dividers*, IEEE Trans. Nucl. Sci., 3, **43**, (1996), 1656-1660
 - [7] S. Argiro, et al., *Passive and Active PMT Biasing Networks II - GAP-99-015*, 1999
 - [8] J.-L. Almein and P. Volkov, *Achieving high rates with CsI(Tl)-Photomultiplier detectors*, IEEE Trans. Nucl. Sci., 1, 36, (1989), 420-425
 - [9] J. Pouthas et al., *The electronics of the INDRA 4p detection array*, Nucl. Instr. Meth. Phy. Res., **A369**, (1996), 222-247
 - [10] J. Pouthas et al., *INDRA, a 4p charged product detection array at GANIL*, Nucl. Instr. Meth. Phy. Res., **A357**, (1995), 418-442

APPENDIX A: HIGH VOLTAGE SPECIFICATIONS

Input voltage	+12 V
Output voltage	+2 kV
Output current	used bias current: 100 μ A max
Total power consumption	< 500 mW, including the output current, the losses and the monitoring
Ripple	Better than 2×10^{-5} full load
Stability	Better than 10^{-4} / $^{\circ}$ C
Remote programing	analog (0 to +2.5 V)
Monitor voltage	analog (0 to +5 V)
Protection	<ul style="list-style-type: none">– short circuit and arc protected– against humidity
Temperature range	<ul style="list-style-type: none">– operating: 0 to 60$^{\circ}$C– storage: -10 to 70$^{\circ}$C
Electromagnetic compatibility	<ul style="list-style-type: none">– very low EMI/RFI emission– one-piece shielding with several connections to the ground
Reliability	The system has to work continuously for more than 10 years